High Frequency Fatigue Crack Propagation Behavior of a Nickel-Base Turbine Disk Alloy

S.A. Padula II, A. Shyam, R.O. Ritchie, and W.W. Milligan

S.A. Padula II, Graduate Student
A. Shyam, Graduate Student
W.W. Milligan, Professor

Department of Metallurgical and Materials Engineering
Michigan Technological University
Houghton, MI 49931

R.O. Ritchie, Professor

Department of Materials Science and Mineral Engineering
University of California
Berkeley, CA 94720

Contact: Walter W. Milligan
(906) 487-2015, Fax (906) 487-2934
e-mail: milligan@mtu.edu

Submitted to

International Journal of Fatigue

12/7/98

ABSTRACT

Fatigue crack propagation tests were conducted on the powder metallurgy nickel-base superalloy KM4 at room temperature. Two different heat treatments were investigated, one which produced a relatively coarse grain size around 55 μm, and another which produced a very fine grain size around 6 μm. Tests were conducted at 50 Hz, and in an advanced servohydraulic testing machine at 1,000 Hz, at R-ratios of 0.4 and 0.7. There was no effect of frequency on the fatigue behavior at room temperature, which is expected in this type of alloy, and this result yields confidence in the reliability of the servohydraulic fatigue testing system. The threshold stress intensity for fatigue crack propagation decreased with decreasing grain size and with increasing R-ratio, again as expected. With increasing grain size, the crack path tortuosity and the crystallographic facet size on the fracture surface both increased substantially, leading to increases in roughness-induced closure and a higher apparent threshold. The threshold ΔK values measured at 10^{-10} m/cycle corresponded to essentially infinite lifetimes, as very small decreases in ΔK from the threshold values resulted in complete crack arrest, and led to difficulty in re-starting the crack growth at higher ΔK levels. Finally, comparisons of the observed thresholds with existing models revealed significant discrepancies between the predicted and measured values.

I. INTRODUCTION

Nickel-base superalloys are high performance materials subject to severe operating conditions in the high temperature turbine section of gas turbine engines. Turbine blades in modern engines are fabricated from Ni-base alloy single crystals which are strengthened by ordered γ' precipitates. Turbine discs are made from polycrystalline Ni-base alloys because these components have less stringent creep resistance requirements (due to lower temperatures) but higher strength requirements (due to higher stresses).

Damage-tolerant design philosophies have allowed the calculation of residual life in turbine disks, by assuming a flaw exists in a critical location which is as large as can be reliably detected by non-destructive inspection techniques. The predicted lifetime is then calculated by integrating the da/dN vs ΔK curve from this assumed flaw size.[1] This approach works well for low cycle fatigue (LCF) loading, and has been an unqualified success at reducing LCF failures while at the same time extending the useful lives of critical components. With these advances, the most common cause of military engine component failures is now high cycle fatigue (HCF).[2] These incidents are related to engine vibrations, and are therefore typically found at very high frequencies (in the kHz range), as well as low stress amplitudes and high R-ratios. No design methodology exists for these types of failures, since they often initiate from a damage site such as a manufacturing defect, fretting defect, foreign object damage, and involve small fatigue crack propagation at very high frequency.[2] This results in very short lives, in terms of time to failure, even at crack propagation velocities near the typical threshold rates of 10^{-10} m/cycle.[3] Therefore, a design philosophy which would be useful in this regime would be based on fatigue crack propagation thresholds. This project, which is part of the Air Force Multi-University Research Initiative (MURI) on High Cycle Fatigue, is aimed at studies of this type in the nickel-base turbine components of military engines. In an earlier paper,[3] similar studies of a titanium compressor alloy were reported. Some of the important issues in high cycle fatigue, including the interaction of small or short cracks with microstructure, are discussed in the earlier report.[3] This paper gives results on a turbine disk alloy at room temperature, while future research will focus on

high temperature behavior in both disk alloys and single crystal blade alloys. Effects of temperature, frequency, microstructure, and damage state will be evaluated.

II. MATERIAL

The turbine disk material studied in this program was the alloy designated KM4,[4] developed by GE Aircraft Engines and Pratt & Whitney. It is a powder metallurgy alloy, which is consolidated by hot extrusion and then forged. Like all nickel-base superalloys, KM4 is strengthened by the formation of γ' precipitates based on Ni_3Al. The nominal composition of the alloy is given in Table 1, and a detailed report of its microstructure and deformation behavior is given elsewhere.[5] All specimens studied in this program were cut from a turbine disk forging that was heat treated by GE Aircraft Engines.

The material is typically heat treated in two different ways.[6] If it is solution treated above the γ' solvus temperature, all the γ' is dissolved, which allows the grains to grow during the solutionizing treatment. It is then forced-air quenched and aged. The result is a material with a grain size of about 55 μm, as shown in Figure 1(a). This microstructure will be referred to as the "super-solvus" material in the remainder of this paper. If, however, the material is only partially solution treated a few degrees below the γ' solvus, some of the γ' remains undissolved, and this pins the grain boundaries. After quenching and ageing, the grain size is only 6 μm, as shown in Figure 1(b). This will be referred to as the "sub-solvus" material in this paper. The large particles seen in Figure 1(b) are the undissolved γ', which are not present in Figure 1(a). At a finer size scale, both materials contain a bi-modal distribution of γ' particles, with coarse particles on the order of 300 nm and fine particles on the order of 50 nm in size.[5] The super-solvus material contains a slightly higher fraction of γ' within the grains (55% vs. 45%) because of the lack of grain boundary γ'. At 650°C, the super-solvus alloy has a strength of about 1,050 MPa, while the sub-solvus material has a strength of about 1,150 MPa.[5] The difference in strength between room temperature and 650°C is negligible in these types of alloys, and so the room temperature values should be about the same.

III. PROCEDURES FOR HIGH FREQUENCY FCP TESTING

Fatigue crack propagation tests were conducted on an MTS servohydraulic testing machine which was specifically designed for testing at frequencies from 0 to 1,000 Hz. The details of the machine are described elsewhere,[9] but it is noted here that the machine is quite flexible, with dynamic load capacities to 25 kN, and has proven over 18 months to be robust and reliable. Fatigue crack propagation tests were conducted largely in compliance with ASTM E647, on four-point bend bars with the dimensions shown in Figure 2. Four-point bending was chosen because effects of mode-mixity will be examined later in asymmetric four-point bending, and it was desirable to keep the geometry constant. The recommended K-gradient of -0.08 mm^{-1} was utilized, and increasing/decreasing K tests were conducted several times to verify the observed threshold behavior. The K-solution of Tada[7] for pure bending, corrected for finite width, was utilized to calculate stress intensity factors. Plots of da/dN vs. ΔK were obtained using the secant method, per ASTM E647.

In an earlier paper,[8] a capacitive crack opening displacement (COD) gage was described which is capable of measuring COD at 1,000 Hz. The intention was to use this gage to measure crack length in the current project. However, while the gage was capable of measuring COD quite well at 1,000 Hz, it was not possible to use this measurement to reproducibly measure crack length, since the crack length function was highly sensitive to very small changes in measured COD, zero position, and temperature. It was not possible to measure the dynamic compliance due to slight noise in the signals at 1,000 Hz. Therefore, crack lengths were measured by using a Questar telescope with a 2 μm resolution. The entire test was videotaped, and the crack length was measured manually from the videotape. Post-test fractographic measurements verified the Questar crack lengths to a high degree of confidence.

IV. RESULTS AND DISCUSSION

A. *Effects of Frequency*

Sub-solvus KM4 specimens were tested in the Paris regime at 50 and 1,000 Hz at an R-ratio of 0.4. The curves are shown in Figure 3. Within experimental error, the curves are indistinguishable, indicating no effect of frequency at room temperature. This was expected, since nickel-base superalloys do not become highly rate sensitive until temperatures in excess of 700°C,[9] and previous research by our group found almost no frequency effect on the strength of KM4 at 650°C.[5] The major implication of this result is that the newly-developed servohydraulic testing machine gives reliable results at frequencies of 1,000 Hz. Similar results were found for the titanium alloy.[3]

B. *Effects of Microstructure*

Figure 4 shows FCP curves for sub-solvus and super-solvus materials at a frequency of 1 kHz and R = 0.7. It is evident that the Paris slopes were similar (~ 4), but the sub-solvus material had a consistently higher fatigue crack propagation rate (at equivalent ΔK) as well as a lower threshold. The measured threshold values (10^{-10} m/cycle growth rates) at this R-ratio were 6.8 MPa$\sqrt{m}$ (sub-solvus) and 9.9 MPa$\sqrt{m}$ (super-solvus). Decreasing the ΔK level by only 0.1 MPa$\sqrt{m}$ led essentially to crack arrest; no propagation was detected even after 200 million cycles. When this was allowed to occur, it became very difficult to restart the crack, suggesting an oxide-induced "coaxing" phenomenon.[10] This behavior suggests that the measured threshold at 10^{-10} m/cycle is truly a "no growth" ΔK value, and that essentially infinite life would result at constant ΔK levels below the measured values.

The lower threshold and higher FCP rates were observed in the sub-solvus material, which had a grain size an order of magnitude finer than the super-solvus material, as discussed earlier and shown in Figure 1. Optical micrographs of the crack paths in sub-solvus and super-solvus materials are shown in Figure 5. It is evident that there was substantially more crack path tortuosity in the coarse-grained super-solvus material which exhibited a higher threshold and a

lower FCP rate. Measurements of the actual crack length divided by the projected crack length in the Mode I plane resulted in ratios of 1.6 for the super-solvus and 1.2 for the sub-solvus, confirming quantitatively that the crack path tortuosity did increase with grain size. Numerous previous investigators[11-20] have found similar effects of grain size on FCP rates in similar nickel-base superalloys tested at low temperatures. The difference in the FCP behavior with grain size has been attributed to intrinsic factors such as slip reversibility and extrinsic factors such as increases in roughness-induced closure; however, these factors are often interrelated.[18] The large grain size leads to increases in heterogeneity of deformation[12,17] and this heterogeneity leads to better slip reversibility[12,17-19] as well as larger crystallographic facets on the fracture surfaces which leads to more roughness-induced closure.[18] Further, the crack paths become more tortuous and deviate from the Mode I plane.[18] All of these effects combine to reduce the crack growth rates and increase the thresholds as the grain size is increased. Evidence supporting these phenomena in KM4 at 1,000 Hz is clearly present in Figures 5 and 6. Figure 5 shows the increase in crack path tortuosity and the deviation from the Mode I plane, while Figure 6 shows the substantial increase in crystallographic facet size for the larger-grained material. Finally, the super-solvus material exhibited faceted growth up to a high transition ΔK level of 35 MPa$\sqrt{m}$, compared to only 13 MPa$\sqrt{m}$ for the sub-solvus, indicating that non-continuum microstructural effects are playing a larger role in the large-grained material, as would be expected. This high transition ΔK level also explains the relatively larger amount of scatter in the super-solvus data.

C. *Effects of R-Ratio*

The effect of load ratio (R = 0.4 and 0.7) on the fatigue crack propagation behavior at 1,000 Hz is illustrated in Figures 7 and 8, and threshold values are summarized in Table 2. The figures and tables show that the effect of R-ratio is higher in the near-threshold regime of crack growth. The sub-solvus curves show expected behavior, such that an increase in R-ratio gives higher crack growth rates and a lower threshold, which can generally be explained by attendant crack closure effects. The super-solvus material also exhibited a slightly reduced threshold at the higher R-

ratio. However, the super-solvus material displayed anomalous behavior in the ΔK region above threshold, since the crack growth rates at the two different R-ratios are basically indistinguishable. Anomalous crack growth behavior in the Paris regime for super-solvus specimen with increasing R could be a stochastic phenomenon (since there was much more scatter in the data in the super-solvus specimens) or it could be due to the fact that monotonic modes of fracture superimpose on cyclic modes of fracture at higher R-ratios.[25] Crack path tortuosity showed a slight increase as R was increased. The ratio of the actual crack length to projected crack length was 1.45 for R = 0.4 and 1.59 for R = 0.7. This implies that there might be a K_{max} effect on threshold. The K_{max} values increase rapidly as the crack length increases. Since faceted growth is observed well into the regime where Paris-Law is obeyed, higher R-ratios (and hence higher K_{max} values) lead to facilitation of mode-I fracture which in turn shows up as better defined facets in the crack path. This may explain the increase in crack path tortuosity and slightly slower crack growth rates as R increases in the super-solvus specimen.

D. *Intrinsic Thresholds*

It is desirable to obtain the intrinsic threshold ΔK value below which cracks will not propagate, in the absence of extrinsic effects such as crack closure. In our earlier paper[3] it was found that this value could be reliably obtained for a Ti-6-4 alloy by conducting long crack FCP tests at R ~ 0.9. The threshold only increased by about 10% when going from R = 0.92 to R = 0.8, and based on this it is reasonable to assume that the thresholds measured here at R = 0.7 are within 20% or better of the actual intrinsic thresholds. These measured values can be compared to existing theoretical models, as discussed below.

Sadananda and Shahinian[22] gave an expression for threshold stress intensity based on dislocation emission from the crack tip as

$$K_{th} = \frac{\sqrt{2\pi b}}{A} \cdot \left[\frac{\mu}{4\pi(1-\nu)} \cdot \ln\frac{\alpha\rho}{b} + \frac{\mu b}{4\pi(1-\nu)\rho} + \frac{\gamma}{\sqrt{2}b} + \frac{\sigma_{ys}}{2} \right] , \quad (1)$$

where the four terms on the right hand side are respectively contributions from self energy of the dislocation, image force, surface energy of the ledge formed and the friction stress which is taken to be the 0.2% yield stress of the material divided by two. Here μ is the shear modulus, γ is the surface energy, ρ is the dislocation distance from the crack tip, α is the dislocation core constant, **b** is the Burgers vector, ν is Poisson's ratio and A is the orientation factor of the slip plane given by $\cos\left(\frac{\theta}{2}\right)\cdot\sin\left(\frac{\theta}{2}\right)\cdot\cos\left(\frac{3\theta}{2}\right)$, where θ is the angle between the actual crack propagation direction and the pure Mode-I direction. The threshold stress intensity range, ΔK, can be represented in terms of K_{th} as

$$\Delta K_{th} = K_{th}\cdot(1-R). \tag{2}$$

Substituting reasonable values for the superalloy into Equations 1 and 2 gives a predicted threshold ΔK value of 2.3 MPa$\sqrt{m}$ at R = 0.7, which is clearly too low.

Weertman's analysis[23] of intrinsic thresholds consisted of modifying limiting conditions for emission of a dislocation from an atomically sharp Griffith crack. The modifying parameter g describes the degree of ductility (and varies from 0.6 to 1.0, with the latter representing the perfectly brittle case) and is a function of the ratio of the theoretical tensile strength to the theoretical shear strength. The Weertman intrinsic threshold is given by

$$\Delta K_{th} = 2g\left[\frac{2\gamma E}{1-\nu^2}\right]^{1/2}, \tag{3}$$

where E is the Young's modulus, γ is the true surface energy of the solid and ν is Poisson's ratio. Using this approach with reasonable values for the material parameters, the intrinsic threshold for KM4 was predicted to be around 1.7 MPa$\sqrt{m}$. Again, this value is too low.

Finally, Lin and Fine[24] suggested a relation for intrinsic threshold, which involved activation of a source identified by dislocation cell wall at a distance from the crack tip, given by

$$\Delta K_{th} = m\mu b\sqrt{\frac{2\pi}{d}} \quad , \tag{4}$$

where μ is the shear modulus, m is the average orientation factor which varies between 2 and 3 for random polycrystals and **b** is the Burgers vector. This model predicts an intrinsic threshold value of ~1 MPa√m for KM4 and is again an underestimate.

The predicted intrinsic thresholds are given for all three models in comparison with the data in Table 3. It is clearly seen that the models under-predict the actual fatigue threshold. Further, the same trend was found in the earlier report on the Ti-6-4 alloy.[3] Potential reasons for the discrepancies between measured and predicted values are discussed in [3]. It is clear that this is a fruitful area for further research.

V. SUMMARY

KM4, a new generation powder metallurgy turbine disk alloy, behaved in a similar fashion to other alloys in its class. It exhibited a grain size effect on FCP rates and thresholds, such that finer grain sizes led to lower thresholds and higher FCP rates. Further, increasing R-ratios resulted in decreasing thresholds and increasing FCP rates. Fractographic observations were consistent with similar alloys, in that faceted fracture was observed at low ΔK levels and facet size scaled with grain size. The measured thresholds at 10^{-10} m/cycle corresponded to essentially infinite lifetimes, as very small decreases in ΔK from the threshold values resulted in complete crack arrest, and led to difficulty in re-starting the crack growth at higher ΔK levels. Finally, there was no frequency effect on FCP behavior between 50 and 1,000 Hz at room temperature. The main contribution of this research, besides verifying previously-determined crack propagation mechanisms, rates, and microstructural effects in a new alloy, is to show that the results do not change as the frequency increases from 50 Hz to 1,000 Hz. Deformation studies and *in situ* SEM fatigue studies at 2 kHz are currently underway.

ACKNOWLEDGEMENTS

This work was supported by the MURI on “High Cycle Fatigue”, funded at Michigan Technological University by the Air Force Office of Scientific Research, Grant No. F49620-96-1-0478, through a subcontract from the University of California at Berkeley.

REFERENCES

1. S. Suresh, Fatigue of Materials, 2nd Ed., Cambridge University Press, Cambridge, 1998, pp. 13-14.
2. B.A. Cowles, *Int. J. Fracture,* 1996, vol. 80, pp. 147-163.
3. B.L. Boyce, J.P. Campbell, O. Roder, A.W. Thompson, W.W. Milligan, and R.O. Ritchie, "Thresholds for High-Cycle Fatigue in a Turbine Engine Ti-6Al-4V Alloy", *Int. J. Fatigue,* in review.
4. D.D. Krueger et al.: US Patent 5143563, September 1, 1992.
5. S. Sinharoy, P. Virro-Nic, E.A. Oja, and W.W. Milligan, "Deformation Behavior of Two Nickel-Base Turbine Disk Alloys at 650^{o}C", *Metall. Mater. Trans. A*, in review.
6. E.S. Huron, R.L. Casey, M.F. Henry, and D.P. Mourer, in Superalloys 1996, R.D. Kissinger et al, eds., TMS Warrendale PA, 1996, pp. 667-676.
7. H. Tada, P.C. Paris and G.R. Irwin, The Stress Analysis of Cracks Handbook, Del Research Corporation, Hellertown, PA, 1973.
8. J.M. Morgan and W.W. Milligan, in High Cycle Fatigue of Structural Materials, W.O. Soboyejo and T.S. Srivatsan, eds., The Minerals, Metals and Materials Society, Warrendale, PA, 1997, pp. 305-312.
9. G.R. Leverant, M. Gell, and S.W. Hopkins, *Mater. Sci. Eng.,* 8, 1971, pp. 125-133.
10. S. Suresh,G.F. Zamiski, and R.O. Ritchie, *Metall. Trans. A*, 12A, 1981, pp.1435-1443.
11. J. Bartos and S.D. Antolovich, in Fracture 1977, D.M.R. Taplin, ed., Pergamon Press, NY, 1977, pp. 995-1005.
12. S.D. Antolovich and N. Jayaraman, in Fatigue: Environment and Temperature Effects, J.J. Burke and V. Weiss, eds., Plenum Press, NY, 1983, pp. 119-144.
13. L.A. James and W.J. Mills, *Engr. Fract. Mech*., 22, 1985, pp. 797-817.
14. J.E. King, *Metal Sci.,* 16, 1982, pp. 345-355.

15. R.A. Venables, M.A. Hicks, and J.E. King, in Fatigue Crack Growth Threshold Concepts, D.L. Davidson and S. Suresh, eds., The Minerals, Metals and Materials Society, Warrendale, PA, 1984, pp. 341-355.
16. J.L. Yuen and P. Roy, *Scripta Metall.*, 19, 1985, pp. 17-22.
17. B.A. Lerch, N. Jayaraman and S.D. Antolovich, *Mater. Sci. Eng.*, 66, 1984, pp. 151-166.
18. J.E. King, *Mater. Sci. Tech.*, 3, 1987, pp. 750-764.
19. D.D. Krueger, S.D. Antolovich, and R.H. Van Stone, *Metall. Trans. A*, 18A, 1987, pp. 1431-1449.
20. T. Denda, P.L. Britz, and J.K. Tien, *Metall. Trans. A*, 23A, 1992, pp. 519-526.
21. K. Sadananda and A.K. Vasudevan, in Fatigue and Fracture of Ordered Intermetallic Materials II, W.O. Soboyejo, T.S. Srivatsan and R.O. Ritchie, eds., The Minerals, Metals and Materials Society, Warrendale, PA, 1995, pp. 273-286.
22. K. Sadananda and P. Shahinian, *Int. J. Fracture*, 13, 1977, pp. 585-594.
23. J. Weertman, in Mechanics of Fatigue, T. Mura, ed., ASME, NY, 1981, pp. 11-19.
24. G.M. Lin and M.E. Fine, *Scripta Metall.*, 16, 1982, pp. 1249-1254.

Tables

Table 1: Composition of KM4

Element	wt%
Co	18
Cr	12
Mo	4
Al	4
Ti	4
Nb	2
B	0.03
C	0.03
Zr	0.03

Table 2: Measured Threshold Stress Intensity Values (10^{-10} m/cycle)

Heat Treatment	Grain size, μm	σ_y, MPa[1]	ΔK_{th}, MPa√m	
			R=0.4	R=0.7
Sub-solvus	6	1,150	8.4	6.8
Super-solvus	55	1,050	10.3	9.9

[1] Estimated from value measured in [5] at 650°C.

Table 3: Predicted Intrinsic Threshold Values

Model	ΔK_{th}, MPa√m
Sadananda and Shahinian[20]	2.3 (R = 0.7)
Weertman[21]	1.7
Lin and Fine[22]	1

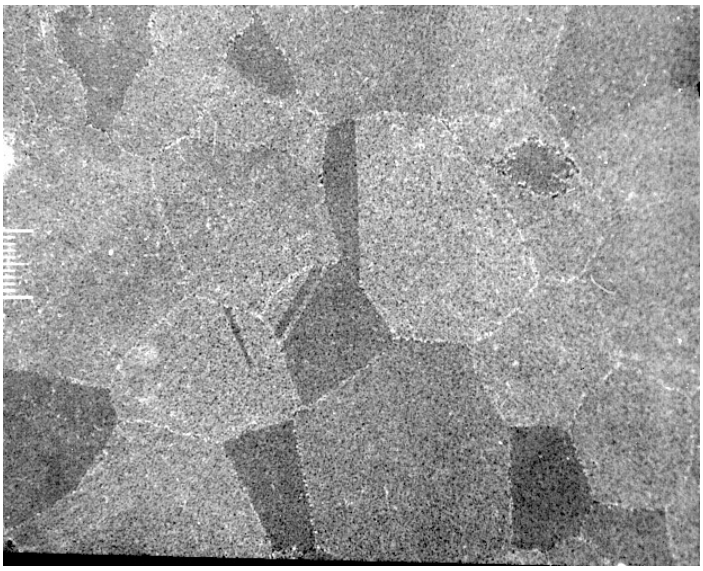

(a)

50 μm

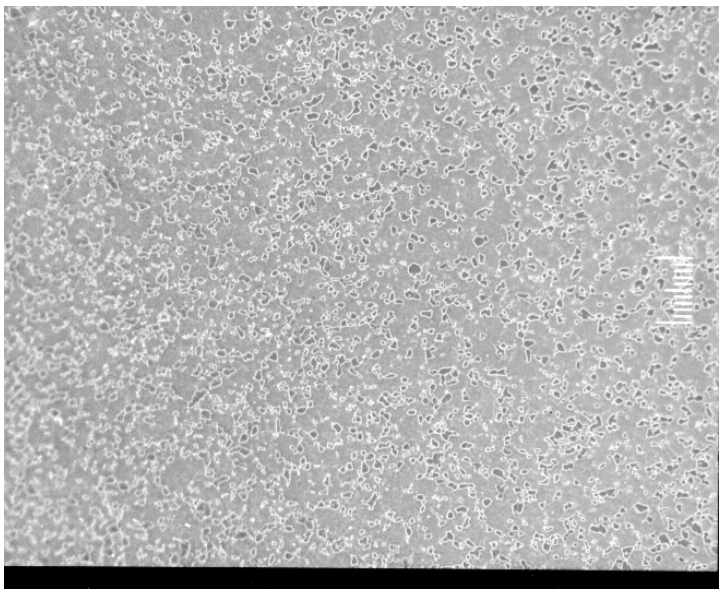

(b)

Figure 1. Optical microstructures of KM4 after heat treatment. (a) Super-solvus heat treatment, showing larger grain size and lack of undissolved γ' precipitates. (b) Sub-solvus heat treatment, showing large γ' particles which did not dissolve during solution treatment. Grain boundaries are not resolved, but are decorated by the large γ' particles. In both cases, finer γ' which is responsible for strengthening is too small to be resolved at this magnification.

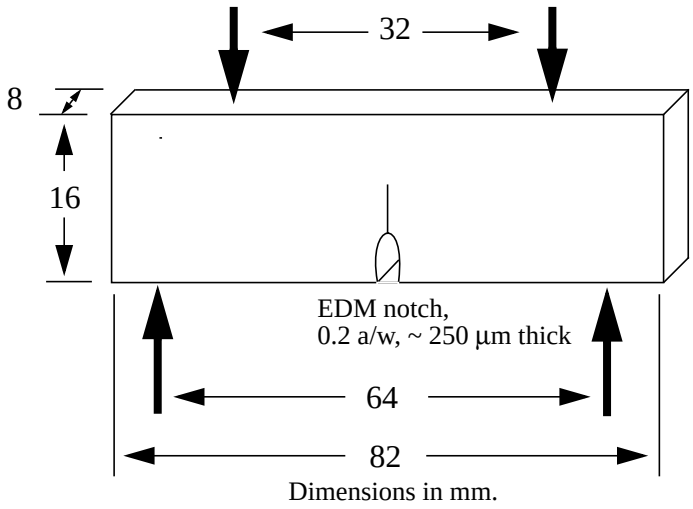

Figure 2. Dimensions of the four-point bend specimens, with loading points indicated.

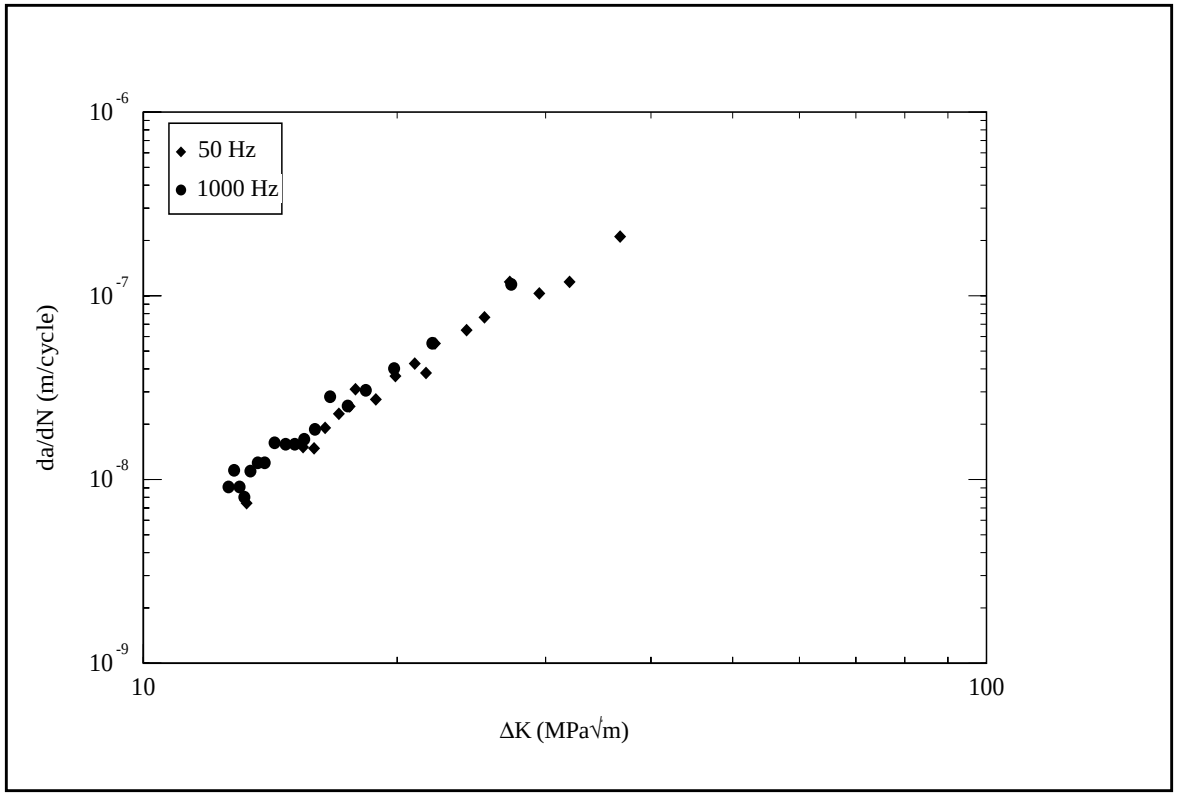

Figure 3. Fatigue crack propagation curves for sub-solvus KM4 in the Paris regime at frequencies of 50 and 1,000 Hz at R = 0.4.

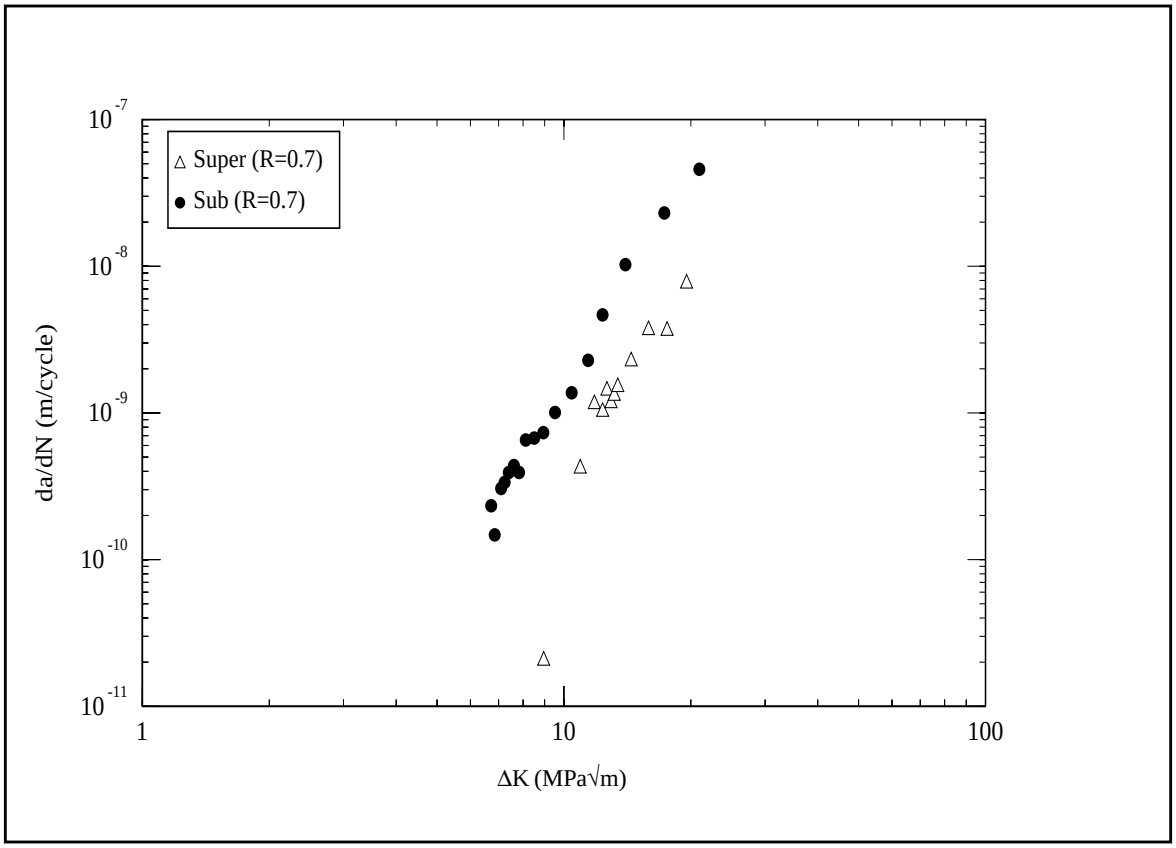

Figure 4. Fatigue crack propagation curves for sub-solvus and super-solvus KM4 in the threshold and early Paris regimes at 1,000 Hz and R = 0.7.

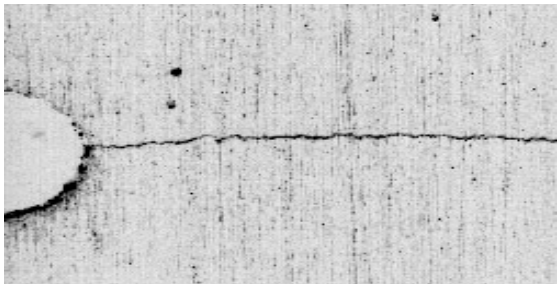

(a)

200 μm

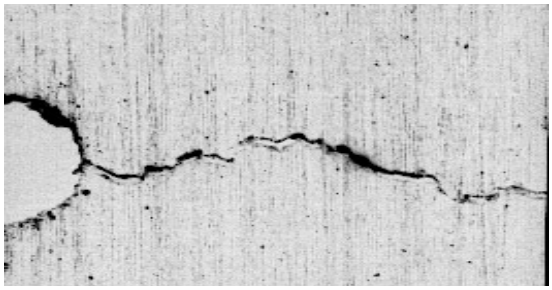

(b)

Figure 5. Optical micrographs of the crack paths in KM4 tested at 1,000 Hz. EDM notches are visible at the left. (a) Sub-solvus material (6 μm grain size), showing relatively planar crack. (b) Super-solvus material (55 μm grain size), showing substantial crack path tortuosity. Crack branching was also observed in the super-solvus material.

(a)

20 μm

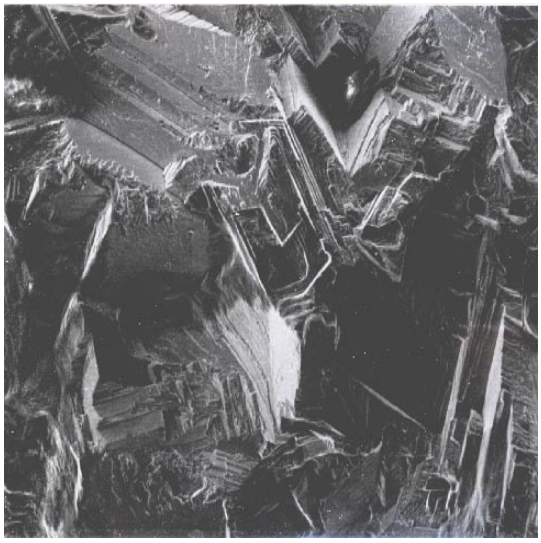

(b)

Figure 6. Scanning Electron Micrographs of the fracture surfaces in the near-threshold regime. KM4 at 1,000 Hz and R = 0.7. (a) Sub-solvus, showing very fine facets. (b) Super-solvus, showing significantly larger crystallographic facets related to the larger grain size.

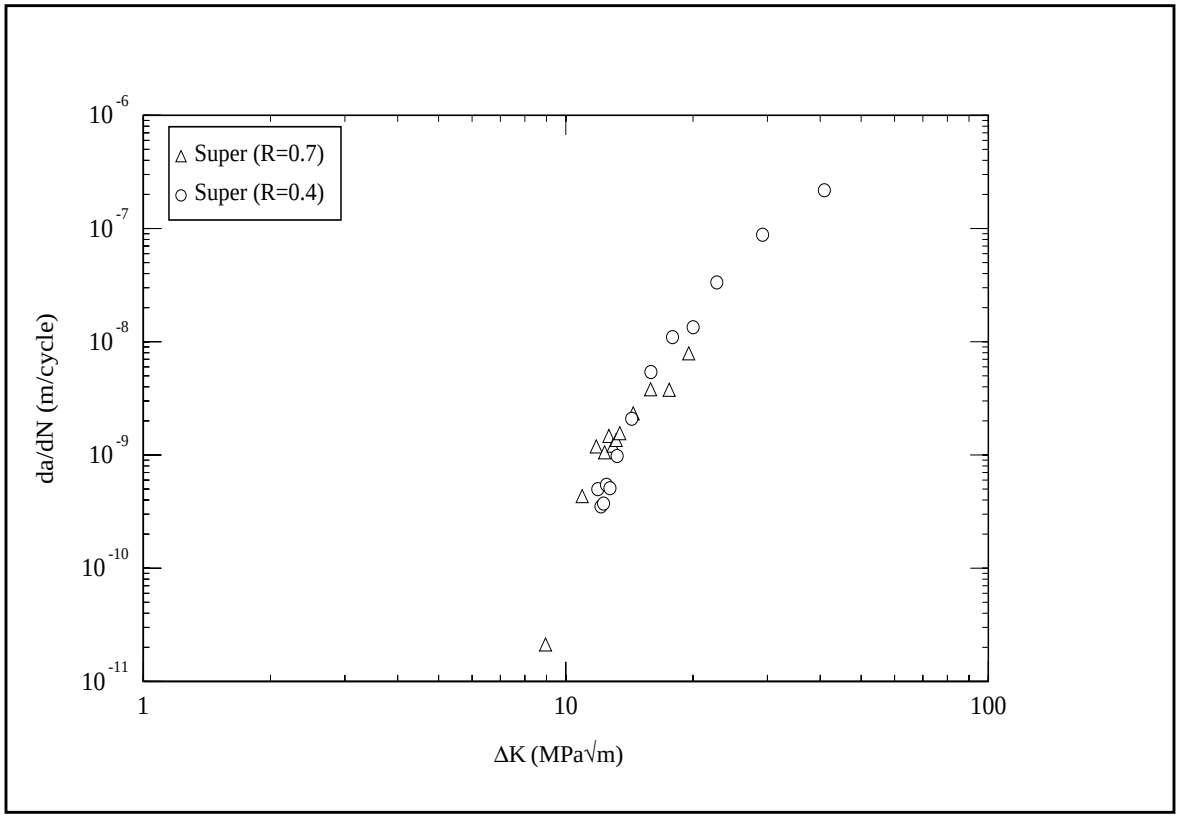

Figure 7. Fatigue crack propagation curves for super-solvus KM4 at 1,000 Hz and two different R-ratios.

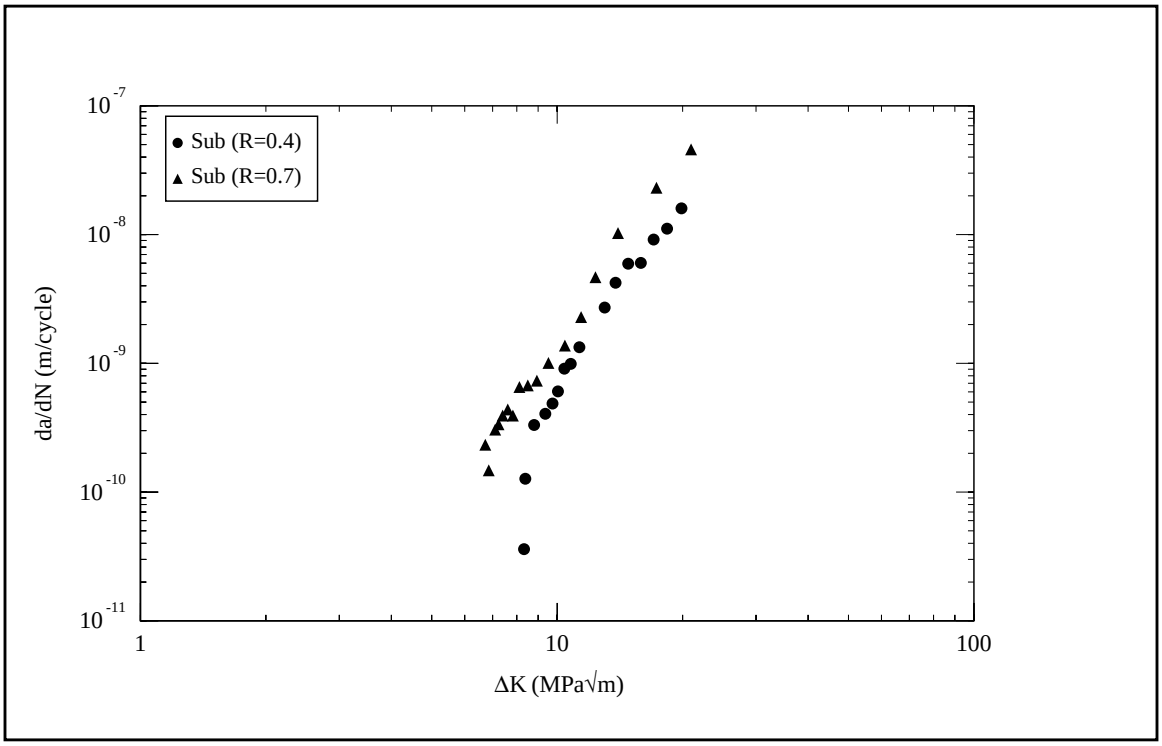

Figure 8. Fatigue crack propagation curves for sub-solvus KM4 at 1,000 Hz and two different R-ratios.